


Force and moment measurements for a generic car model in proximity to a side wall

Proc IMechE Part D:
J Automobile Engineering
226(10) 1352–1364
© Cranfield University, UK 2012
Reprints and permissions:
sagepub.co.uk/journalsPermissions.nav
DOI: 10.1177/0954407012443643
pid.sagepub.com


Russell Strachan¹, Kevin Knowles¹, Nicholas J Lawson² and Mark V Finnis¹

Abstract

Force and moment data are presented for an Ahmed reference model with backlight angles of 10°, 25° and 40° at various distances from a side wall. Tests were run at a freestream velocity of 25 m/s and a rolling road provided ground simulation. Six-component force data were recorded and compared with previous experimental data. It is found that the proximity of the side wall causes a general increase in both the lift coefficient and the pitching moment for the Ahmed model, with the increase in the pitching moment becoming more rapid with decreasing wall distance. Increasing the proximity to the wall is further found to increase the overall Ahmed model drag. Furthermore, there is evidence of the breakdown of longitudinal vortices on the near-wall side of the model as the wall-to-model distance decreases, and a large pressure drop on the near-wall model side. This pressure drop increases in magnitude as the wall-to-model distance decreases, before dissipating at wall distances where the boundary layer restricts the flow.

Keywords

Automotive aerodynamics, Ahmed body, side wall, Type C racecar

Date received: 10 October 2011; accepted: 28 February 2012

Introduction

Ahmed model

The Ahmed reference model was originally developed for a time-averaged vehicle wake investigation.¹ It is a car-like bluff body with a curved fore body, a straight centre section and an angled rear end, representing a highly simplified quarter-scale lower-medium-size hatchback vehicle. The specific angle of the back end can be altered between 0° and 40°, in 5° increments. The model's major dimensions are 1044 mm × 389 mm × 288 mm (length × width × height). A diagram of the Ahmed reference model is shown in Figure 1.

The Ahmed body was designed to have a fully attached flow over the front, and to exhibit many of the flow features of an automobile with its nine interchangeable rear ends. This variation in the backlight geometry provides a range of flow characteristics over the back end of the model.

The geometry of this bluff body was designed to be such that an experiment could be conducted with reference to only one significant aerodynamic feature, namely the flow over the slanted rear end, as the flow was expected to remain attached over the other sections. The Ahmed model has also lent itself well to the

validation of computational fluid dynamics (CFD) codes, as the accuracy of these codes can be determined, once again, with only one significant aerodynamic factor varying between cases. This allows validation to be conducted without the common difficulty that sources of errors from different regions of the flow field cancel each other out. Numerous previous experimental investigations on this model have been reported.^{2–6} These were conducted in various wind tunnels over a range of airspeeds. In general, during testing, the model was supported from underneath by four cylindrical struts attached to a fixed ground plane. The present tests, however, in common with those carried out by Strachan et al.,⁶ were conducted with a moving ground plane, with the model being supported from above by an aerodynamic strut.

¹Aeromechanical Systems Group, Cranfield University, Shrivenham, Wiltshire, UK

²National Flying Laboratory Centre, Cranfield University, Cranfield, Bedfordshire, UK

Corresponding author:

Nicholas J Lawson, National Flying Laboratory Centre, Cranfield University, Cranfield, Bedfordshire MK43 0AL, UK.

Email: n.lawson@cranfield.ac.uk

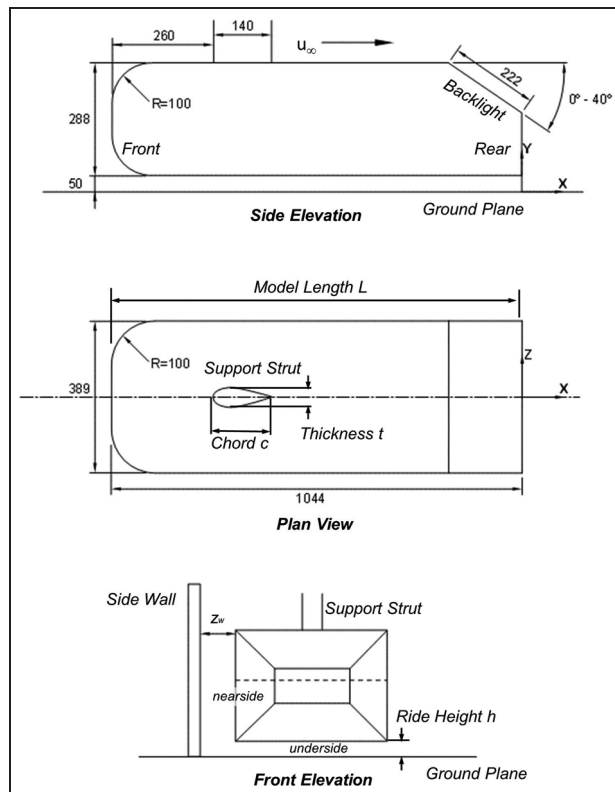


Figure 1. Schematic diagram of the Ahmed reference model (dimensions in millimetres), where the flow is from left to right.

It has been shown that the flow over the angled back section is dependent on the specific backlight angle being investigated.¹ Two critical backlight angles have been found where the flow structure changes significantly. Below 12.5° (the first critical angle), the airflow over the backlight remains fully attached, before separating from the model when it reaches the vertical rear end. The flow from the side walls adjacent to the backlight produces a pair of counter-rotating vortices which continue downstream. For backlight angles between 12.5° and 30° (the second critical angle) the flow over the backlight becomes highly three dimensional. Two counter-rotating lateral vortices are again shed from the sides of the angled rear section but are larger than those formed below 12.5° . This increased vortex size affects the flow over the complete backlight, resulting in the three-dimensional flow. These substantial vortices are also responsible for maintaining the attached flow over a section of the backlight up to an angle of 30° and have been shown to extend more than 500 mm ($0.48 L$) beyond the model's trailing edge. Close to the second critical angle, a separation bubble is formed over the backlight. In this case, the flow separates from the body but re-attaches to the backlight before reaching the vertical rear section. The flow then subsequently separates again from the rear of the model. Above 30° , the flow over the angled section is fully separated, but there remains a weak tendency of the flow to turn around the side edge of the model; this is a result of the relative separation positions of the flow over the top of

the model and that over the backlight side edges. When the flow is in this state, a nearly constant pressure is found across the backlight.

Previous experimental near-wall investigations

There has been a great deal of research performed into discovering the effects of cars running in a slipstream and into the interference effects experienced when a car is passed by another car. To date, however, the interference effects between a car and a retaining wall to which it is often running in very close proximity have not been the subject of equal scrutiny. To the present authors' knowledge, there have been only two experimental investigations performed on the aerodynamic effects experienced by a car when travelling in close proximity to a side wall.^{7,8}

An experimental wall proximity investigation was conducted by Wallis and Quinlan.⁷ In this case, a three-eighths-scale generic National Association for Stock Car Auto Racing (NASCAR) model was tested in proximity to a wall scaled to 1.37 m height ($0.29 L$). The experiment was performed in a closed-section wind tunnel, without moving ground simulation, and no boundary layer control was employed on either the test section floor or the wall itself. The NASCAR model was tested at various distances from the wall, ranging from an equivalent full-size distance of 52 in ($z_w = 0.74 L$) from the near-side car door, to the car virtually touching the wall.

Brown⁸ conducted a wall proximity study employing a simplified Type C racecar model. The tests were conducted in a closed-section wind tunnel, without boundary layer control on the model wall. Ground simulation in the form of a rolling road was employed, with suction upstream of the leading edge of the rolling road being used to remove the tunnel boundary layer. Despite the model's simplicity, it also included a front splitter plate, a rear wing and an underbody diffuser, each of which produced a significant downforce. The model was tested at side-wall distances ranging from approximately $z_w = 0.14 L$ to $z_w = 0.01 L$ at various ride heights. The model was also tested with various rear wing angles of attack and with a range of Reynolds numbers.

Experiments and techniques

Experimental set-up

With reference to Figure 1, the model was mounted 50 mm ($0.048 L$) above a moving ground plane and supported from above by an aerodynamic strut ($t/c = 0.25$, positioned $0.25 L$ downstream of the leading edge). Measurements of the six forces and moments were taken using a load cell mounted inside the model.

Wind tunnel

The model was tested in the 'D.S. Houghton' open-jet closed-return wind tunnel at Cranfield University,

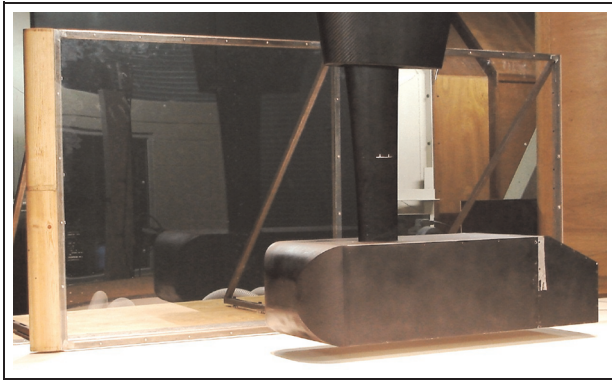


Figure 2. Photograph of the Ahmed reference model and wall mounted in the wind tunnel.

Shrivenham. This has nozzle dimensions of 2.74 m wide by 1.66 m high. A continuous-belt rolling road (1 m wide by 3.5 m long) provided moving ground simulation. Throughout the testing, the freestream velocity was constant at 25 m/s, corresponding to a Reynolds number Re of approximately 1.7×10^6 (based on the model length L). The rolling road was synchronised with the tunnel freestream velocity, and boundary layer control was provided by upstream suction and a knife-edge transition. The system achieved an onset boundary layer thickness of 1 mm (to 99% freestream dynamic pressure) and a freestream turbulence intensity below 0.25%. Strachan et al.⁶ have previously outlined the basic wind tunnel set-up in more detail.

The backlight of the model was designed so as to be interchangeable with a plate containing 800 pressure tappings. A total of 32 rows of tappings were equispaced about the longitudinal axes of the backlight with a higher concentration of tappings close to the edges of the backlight. This arrangement allowed the study of the backlight vortex structure and the effects of the wall. The tappings were read sequentially, each averaged over a period of 16 s, at a rate of 500 Hz. Pressure measurements were conducted for only the 25° case, both for the isolated model and in the proximity of the wall.

With reference to Figure 2, the vertical wall was mounted 2 mm above the surface of the rolling road using a series of right-angle joints. The wall was made from Perspex so as to minimise any reflections for laser Doppler anemometry data acquisition and contained a radiused leading edge to prevent flow separation. The model wall extended $0.5L$ upstream and $0.5L$ downstream of the leading edge and the trailing edge respectively of the Ahmed model, and extended to a height of $0.63L$ above the top edge of the model.

Results and discussion

Ahmed model results

Figures 3 and 4 plot the variation in the lift coefficient C_L and the variation in the pitching moment coefficient

C_M , respectively, with changing wall distance for the 10°, 25° and 40° Ahmed models. Values are plotted as variations from the equivalent isolated no-wall model cases. There is found to be a fall in the lift coefficient between the isolated and $z_w = 0.287L$ cases for all model geometries and ride heights tested. It is also clear from Figure 3 that at a certain wall distance, which varies with the model geometry, C_L increases rapidly and continues to do so as the wall distance decreases further. Therefore, the wall proximity causes a larger drop in C_p underneath the model than on top of the model, with a corresponding overall decrease in C_L . The wall distances at which the lift has reached a level above that measured on the isolated model are in the ranges $(0.068\text{--}0.083)z_w/L$ for the 10° backlight angle, $(0.088\text{--}0.187)z_w/L$ for the 25° backlight angle and $(0.043\text{--}0.046)z_w/L$ for the 40° backlight angle. Two wall distances are given for the 25° backlight angle as the results suggest that this value is dependent on the ride height h . It appears, therefore, that the wall distance has the greatest effect on the 25° backlight model. This is confirmed by analysing the overall increase in C_L between the isolated model and the smallest wall distance for each backlight angle, for the extremes of the recorded ride heights. The 10° backlight model experiences a rise in C_L of approximately 0.156 between these two wall distances at a 30 mm ride height, and just over half this increase (0.084) at a 70 mm ride height. The 25° backlight model experiences a greater increase in C_L of approximately 0.264 at a 30 mm ride height to a C_L increase of 0.17 at a 70 mm ride height. Finally, the 40° backlight model experiences the smallest increase in C_L of 0.144 at a 30 mm ride height and 0.064 at a 70 mm ride height. Hence the decrease in the wall distance lowers the pressure in the region of the 25° backlight by a greater amount than for either the 10° backlight or the 40° backlight. It is also seen from these results that there exists a more rapid increase in C_L with decreasing ride height and that this is the case for all the backlight angles tested. Owing to the separated flow over the 40° model, it must therefore be concluded that this effect is a result of the pressure drop over the front end and top of the model, rather than over the backlight.

As the wall distance falls, the pressure drop over the 25° backlight is greater than the corresponding drop over either the 10° backlight or the 40° backlight. This results in a larger overall increase in C_L when compared with the isolated model case. Owing to the relatively long middle section of the model, any relationship between the flow over the front and rear ends of the model should have only a minor effect. As such, the decreases in C_p over the front-end suction peak with decreasing wall distance are almost equal for the three tested model configurations. As there is a larger decrease in C_p over the 25° rear end, this corresponds to an overall increase in C_M between the isolated model and near-wall cases at this backlight angle. Furthermore, there is a smaller increase in C_M over the

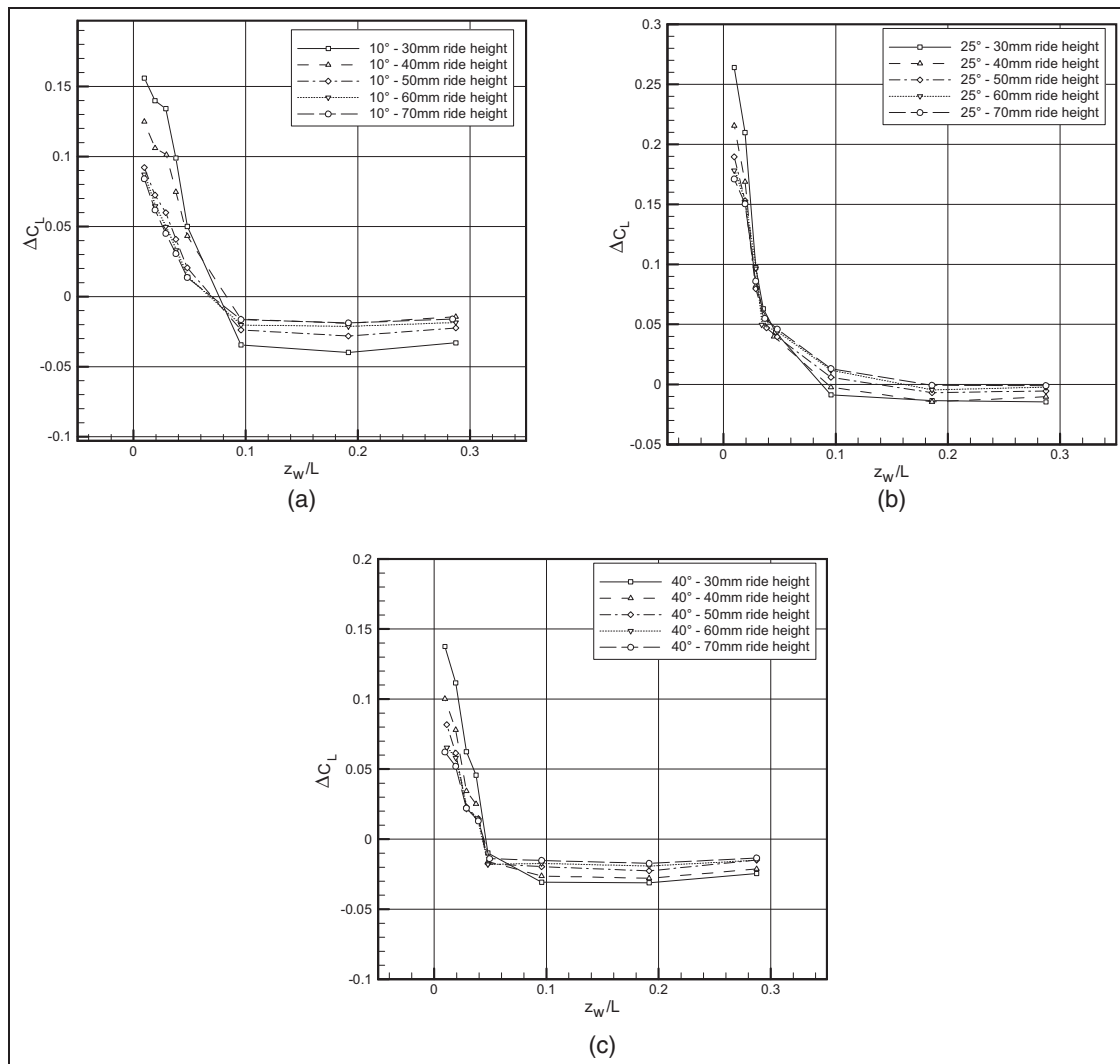


Figure 3. Variation in C_L for the Ahmed model with the proximity of the side wall from the equivalent isolated model case: (a) 10° ; (b) 25° ; (c) 40° .

10° model than over the 40° model, owing to the lower pressure drop over the 40° back end, caused by the separated backlight flow at this larger angle. To analyse this effect further, we consider the plots of C_M against the wall distance shown in Figure 4. In this case, for the 10° backlight model with a 30 mm ride height, there is an overall increase in C_M of 0.091 between the isolated model and near-wall results, with corresponding increases of 0.059 and 0.101 over the 25° model and the 40° model, respectively. At a ride height of 70 mm this trend is continued with a rise in C_M of 0.06 over the 10° model, 0.041 over the 25° model, and 0.075 over the 40° model. This confirms the general insensitivity of C_M to the backlight angle and the ride height.

Figure 5 plots the variation in C_D against the change in the wall distance for a range of model ride heights. General results show an increase in C_D with decreasing wall distance for the three model geometries. Between the isolated model and near-wall cases, for a 30 mm ride height, there is an increase in C_D of 0.142 for the 10°

model, 0.111 for the 25° model, and 0.134 for the 40° backlight model. This increase in C_D with the 25° backlight is consistent with a peak in C_L and C_D reported from the corresponding isolated model results.⁶ Given the fact that the lift and drag characteristics in the isolated model are dominated by the behaviour of the flow in the backlight area, this result indicates that the wall has the greatest effect on the backlight pressure distribution and flow separation and less effect on the model front. As the backlight flow behaviour is strongly related to the behaviour of the backlight vortex pair,^{5,6} the presence of the wall will modify this vortex pair behaviour, resulting in an increase in the drag for all the wall cases. The increase in the drag will be caused by a reduction in the effectiveness of the vortex pair to maintain attached flow in the backlight area, with a corresponding increase in the pressure drag. This reduced effectiveness is caused by a weaker backlight vortex adjacent to the wall due to the presence of the wall.^{5,6}

Figure 6 plots the variation in the side-force coefficient with the wall distance for the three model

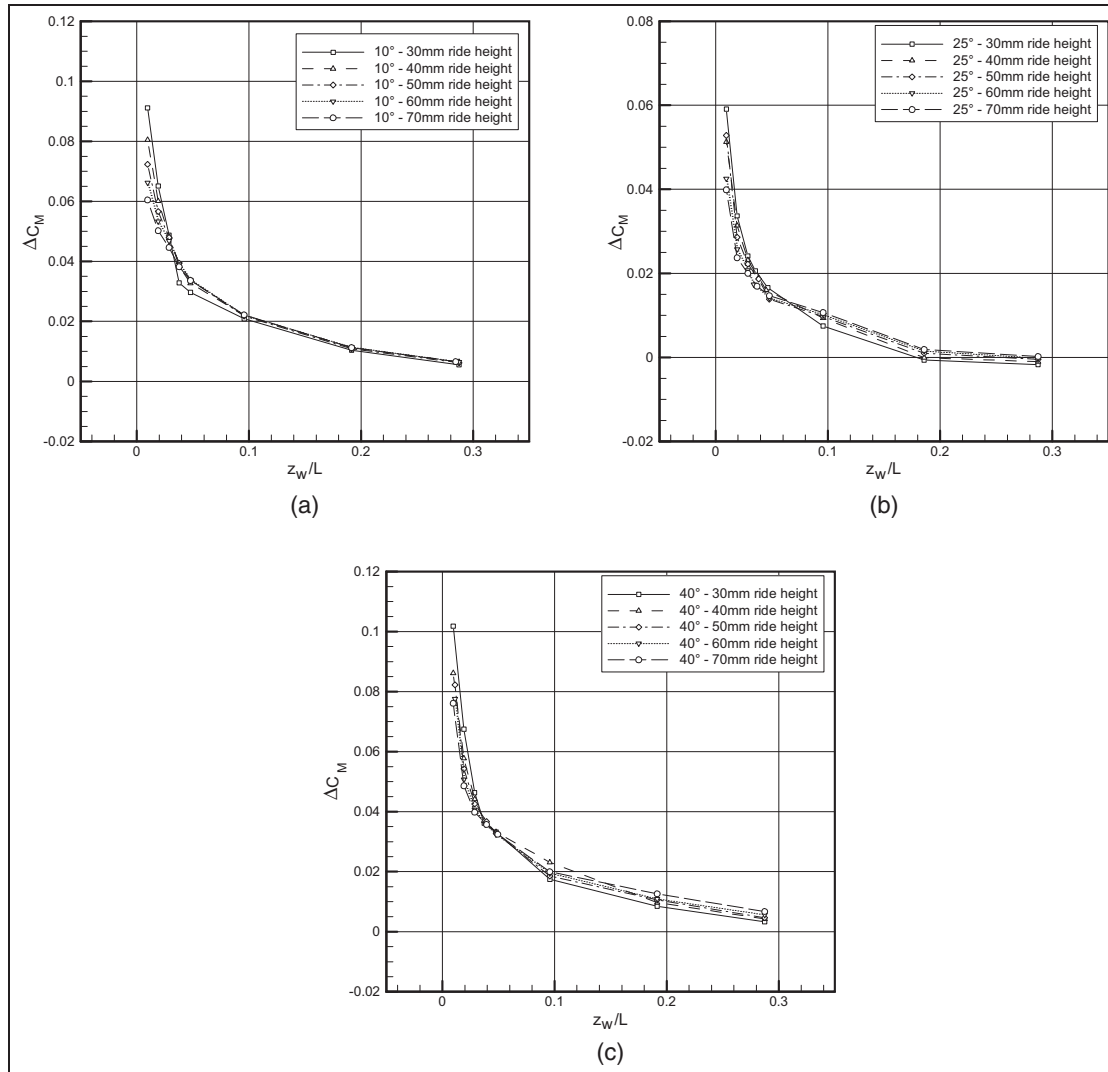


Figure 4. Variation in C_M for the Ahmed model with the proximity of the side wall from the equivalent isolated model case: (a) 10° ; (b) 25° ; (c) 40° .

configurations, with positive values of C_Z corresponding to a force towards the side wall. For all model configurations, ride heights and wall distances tested, there remains a positive value of C_Z . Figure 6 also shows that, for each of the three backlight angles and at almost all the recorded ride heights, there exists a maximum C_Z at $z_w = 0.029L$. Following this maximum, there is a decrease in C_Z consistent with a $1/(z_w/L)$ relationship towards zero force at infinity, i.e. the isolated model case. This positive side force is a result of the pressure drop between the side of the model and the wall with decreasing distance and is similar to the effect observed for the variation in C_L with decreasing ride height. The sharp decrease in C_Z close to the wall was not shown to cause a negative side force at any of the wall distances measured. However, in the extreme case when the model touches the wall, it is expected that there will be a point where the side force acts away from the wall.

The sudden drop in C_Z and the corresponding side force are attributed to the interaction of the wall and

model boundary layers and to restriction of the flow by the resultant pressure distribution. This interaction is evident if we consider the boundary layer thicknesses of the model and wall in isolation. For example, based on flat-plate turbulent boundary layer theory,⁹ the boundary layer thickness on the wall adjacent to the rear of the model in the absence of the wall would be 29 mm. Similarly, the adjacent boundary layer thickness on the side of the model in the absence of the wall is estimated to be 21 mm. Thus, the peak in C_Z at around $z_w = 0.03L$ for all cases, or around a gap of 30 mm between the wall and the model, is of the same order of magnitude as these isolated boundary layer thicknesses towards the rear of the model.

Attention must also be paid to the geometry of the front end of the model. The increased suction between the wall and the near side of the model will relocate the stagnation point on the front of the model closer to the wall. Owing to the shape of the model this increase in the pressure causes a negative side force away from the wall. This force increase is greater than the resulting

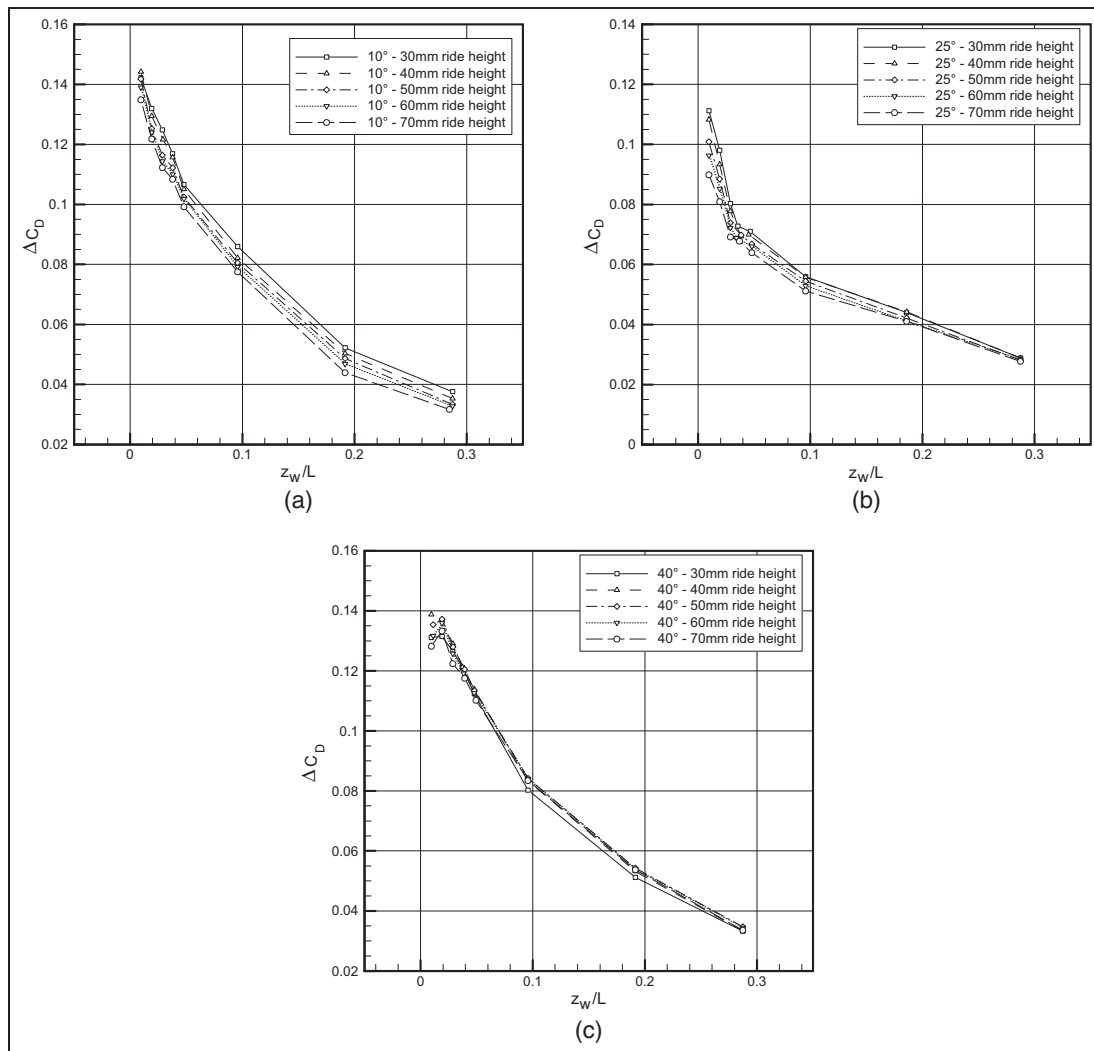


Figure 5. Variation in C_D for the Ahmed model with the proximity of the side wall from the equivalent isolated model case: (a) 10°; (b) 25°; (c) 40°.

pressure drop over the off side of the front end, resulting in an overall negative C_Z contribution from this section of the model. From the plots, it is clear that this effect is less significant than the afore mentioned pressure drop over the near side of the model but nonetheless must be considered during analysis. The maximum value of C_Z was found to be 0.31 in the 10° case, 0.38 in the 25° case, and 0.27 in the 40° case. The higher value of C_Z in the 25° case is most probably a result of the lower pressure at the rear-end suction peak. This effect will cause a larger pressure drop over the near side of the model.

With reference to Figure 7, the plots of C_N against the wall distance in general exhibit a decrease in the yawing moment with increasing wall distance approximately consistent with a $1/(z_w/L)$ relationship, i.e. similar to the C_Z relationship. Nearer the wall, i.e. $z_w < 0.05L$, the characteristic becomes more complex with a reduction in C_N before rising again as the model is brought closer to the side wall. The exact point at which this kink occurs is located closer to the wall with decreasing ride height. There also exists a large increase

in C_N between $z_w = 0.019L$ and $z_w = 0.001L$ for the 10° and 40° cases, which is not mirrored by the 25° case. Closer inspection, however, reveals that, despite the large variations in C_N between the three model geometries at $z_w = 0.019L$ (up to 0.02, or 50% of the overall values), the variations at $z_w = 0.001L$ are found to be only around 0.004, now around 6% of the overall values. At this stage, as this kink in the data occurs for all cases with a wall model gap of around 50mm, as in the previous results of C_Z , it is thought that this characteristic is related to the interaction of the side-wall boundary layer with the model boundary layer. More detailed measurements, such as outlined by Strachan et al.,⁵ would help to confirm this.

The variation in the rolling moment coefficient C_R with the wall distance z_w , for all the model configurations tested, is plotted in Figure 8. There are three areas on the model which have significant effects on C_R . First, the increased pressure over the near-side section of the front end of the model is skewed towards the ground plane as a result of the lowered pressure over the top of the model, subsequently imparting a negative

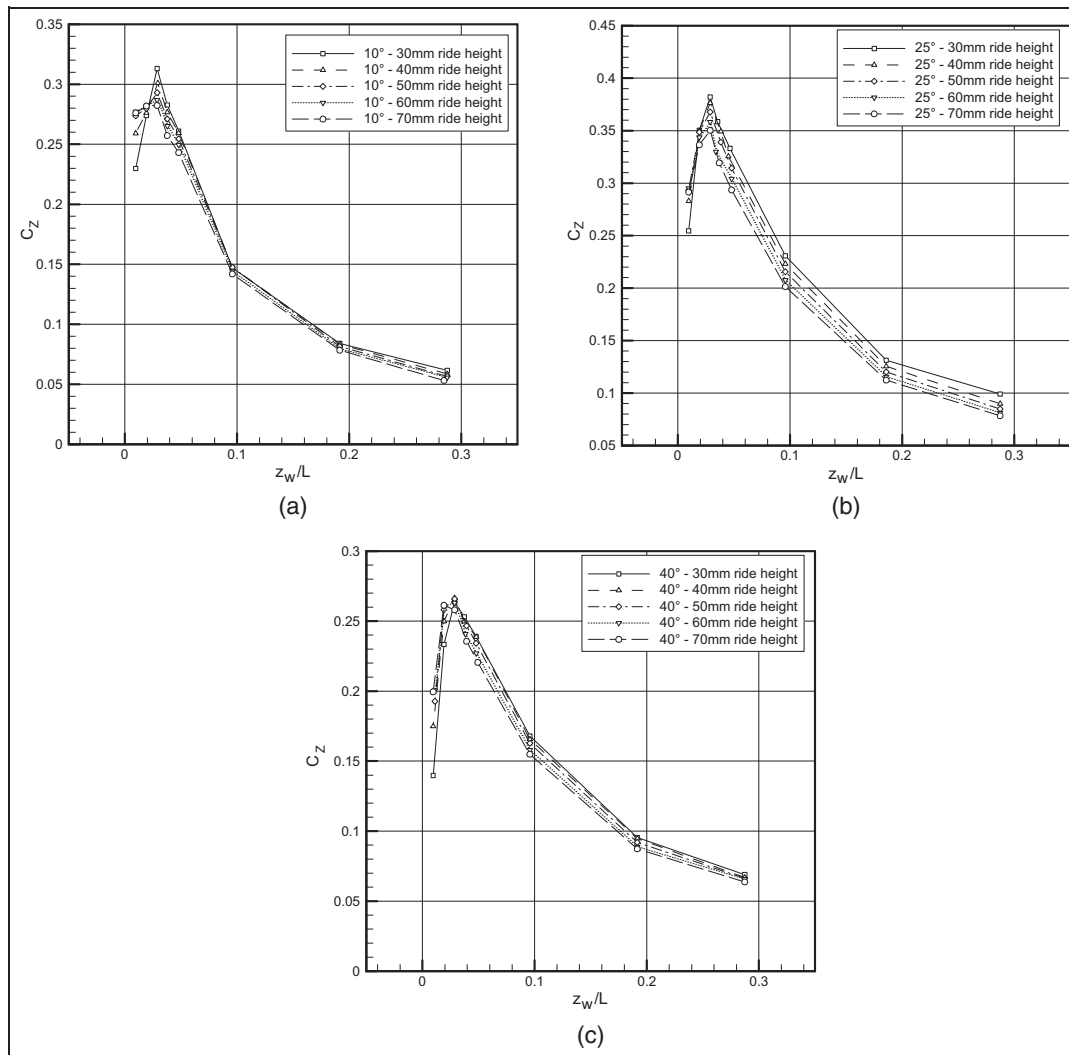


Figure 6. Variation in C_z for the Ahmed model with the proximity of the side wall: (a) 10° ; (b) 25° ; (c) 40° .

(clockwise, if looking from behind the model) rolling moment. Second, the lower pressure over the top of the model is skewed towards the near side, resulting in a positive rolling moment. Third, the pressure drop over the near side of the model is skewed towards the top of the model, as a result of the lower pressure in that region. This contributes a negative rolling moment to the model. Previous computational analysis over the 25° backlight⁵ also showed significant variation in the pressure with the wall distance very close to the model sides as a result of the change in the longitudinal vortex strength, as similarly found in the C_D results discussed previously. As the near-side vortex was found to decrease in strength with the subsequent increase in pressure over the model and the opposite effect on the off-side vortex, the net result is a positive rolling moment on the model. As the strength of these vortices at 25° was shown to be far greater than their counterparts on the 10° model and as they are not formed over the 40° model, any discernible effect that they may have on C_R will be found in the 25° model results. However, even in the case of the 25° model, these effects will not

contribute a large rolling moment in terms of C_R for the overall model.

It can be seen from Figure 8 that, with one exception, there was a negative rolling moment on the model. This suggests that, in general, the increased pressure over the front end and the pressure drop over the near side have greater effects on the rolling moment than the pressure drop over the top of the model does. It is also clear, however, that at a wall distance of $0.029L$ there exists in every tested configuration a minimum C_R and, as the wall distance falls further, there is a significant increase in the rolling moment (i.e. a reduction in the negative rolling moment). Referring back to the plots of C_z (Figure 6), it was shown that at a wall distance of $0.029L$ there was evidence that the boundary layers on the model and wall restrict the flow between them. This would lead, first, to the previously discussed drop in suction between the wall and the model and, second, to a drop in the pressure over the near-side section of the model's front end. As a result, there is a significant shift not only in the side force but also in the rolling moment.

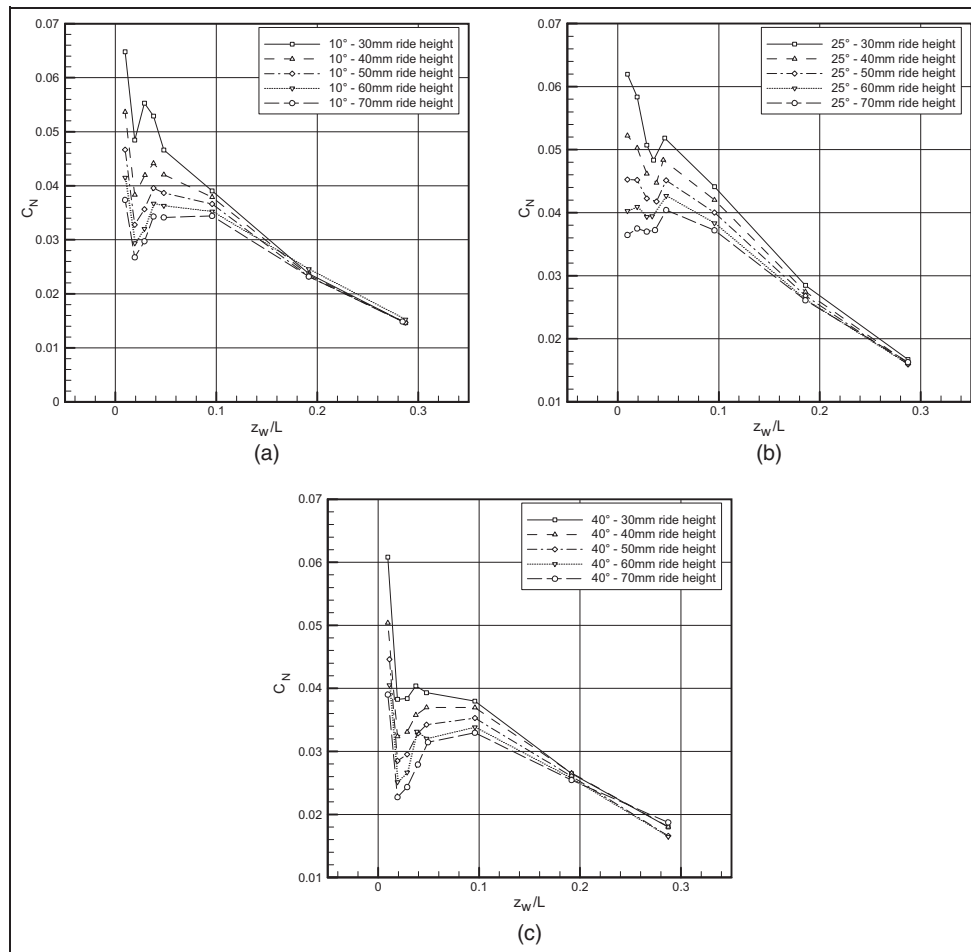


Figure 7. Variation in C_N for the Ahmed model with the proximity of the side wall: (a) 10° ; (b) 25° ; (c) 40° .

It is also clear from Figure 8 that the minimum values of C_R are also significantly influenced by the backlight angle of the model. Indeed, these are found to be -0.017 for the 10° model, -0.024 for the 25° model, and -0.0145 for the 40° model, in each case the results being taken for the 70 mm ride height cases, where these minima are lowest. Referring again to the plots of C_Z against the wall distance in Figure 6, these variations between the backlight angles can be explained. It was found that there was a similar variation in the maximum levels of the side force between the three model configurations. This again corresponds to the greater suction between the wall and the 25° model than between the wall and either the 10° model or the 40° model. This has an effect on the overall rolling moment. As such, the minimum rolling moment for the 25° case is lower than for the 10° case, which is again lower than for the 40° case.

Summary of the Ahmed model force and moment results

The following provides an overview of the variations in the aerodynamic forces and moments experienced by the Ahmed model with decreasing wall distance.

1. C_L drops slightly as the model approaches the wall, as a result of increased suction under the model. At smaller wall distances, however, the increased suction over the top of the model's front end becomes dominant in the variation in the lift, causing a rapid increase in C_L when the wall is in close proximity.
2. C_D increases with decreasing wall distance for all the configurations tested and this is related to the modification of the backlight vortex pair and the corresponding backlight pressure drag, by the presence of the wall.
3. C_Z acts towards the side wall for all the configurations tested. However, the increase in the side force with decreasing wall distance reaches a maximum point before experiencing a rapid decrease. This is thought to arise because the boundary layers restrict the flow between the wall and the model at small distances.
4. C_M increases with decreasing wall distance for all the cases tested, owing to the concentration of the pressure drop over the top of the model near the leading edge. At the closest wall distances measured, where the drop in the pressure over the top of the model is greater than that on the underside

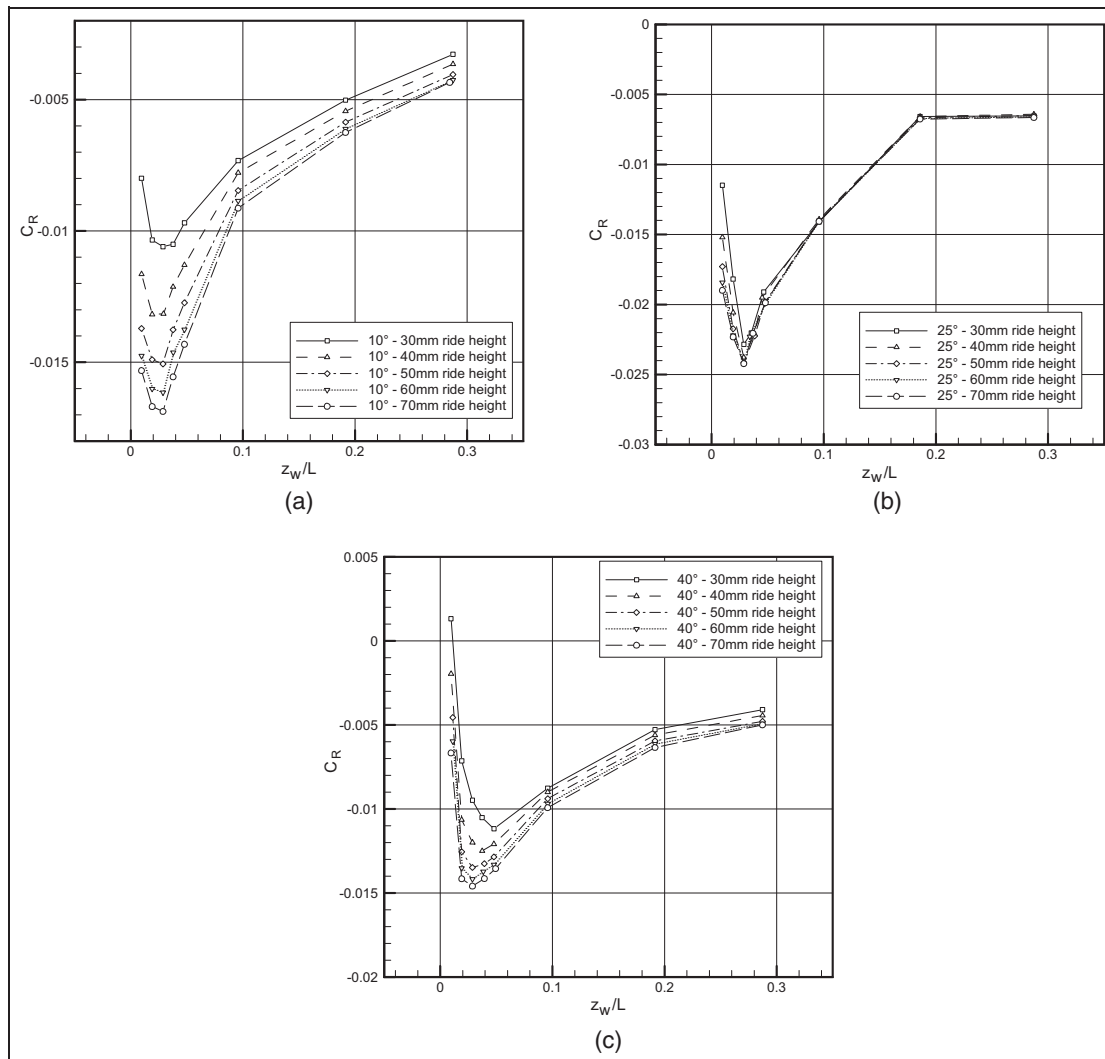


Figure 8. Variation in C_R for the Ahmed model with the proximity of the side wall: (a) 10°; (b) 25°; (c) 40°.

(causing the increase in C_L), C_M experiences a more rapid increase.

5. C_N is found to be positive (nose away from the wall) in all the tests conducted. This is a result of the increase in C_p on the lower near-side section of the model's front end. This change in C_p is the dominant factor in the overall value of C_N for all the wall distances tested.
6. C_R decreases with falling wall distance up to a point. At smaller wall distances, where the boundary layer growth on the near side of the body and on the side wall has restricted the flow between the model and wall, C_R begins to increase rapidly. In this case, both the high pressure over the near side of the front end and the pressure drop over the near side fall.

Comparison with previous studies

To assess the generality of the Ahmed model near-wall results, the following data will be compared directly with those obtained by Brown.⁸ This experimental

study used a Type C racecar model above a moving ground plane and a side wall of the model without boundary layer control. The flow around the Type C model differs significantly from that around the Ahmed model. Firstly, the model has a sharp leading edge and front splitter (Figure 9), causing the formation of leading-edge vortices. There is also a 10° diffuser on the Type C model, which adds a significant rear-end downforce. The addition of the rear wing also adds a rear-end downforce which was not experienced by the Ahmed model body. Furthermore, the Type C model is significantly wider than the Ahmed model (506 mm in comparison with 389 mm), while also being of similar overall length (1123 mm in comparison with 1044 mm for the Ahmed model). It is therefore expected that proximity of the wall will cause a greater pressure drop over the off-side top and bottom of the model when compared with the Ahmed model and wall.

As more detailed data are available from the 25° Ahmed model and given that the flow over the rear diffuser on the Type C model more closely resembles that over the Ahmed model 25° backlight, the 25° Ahmed

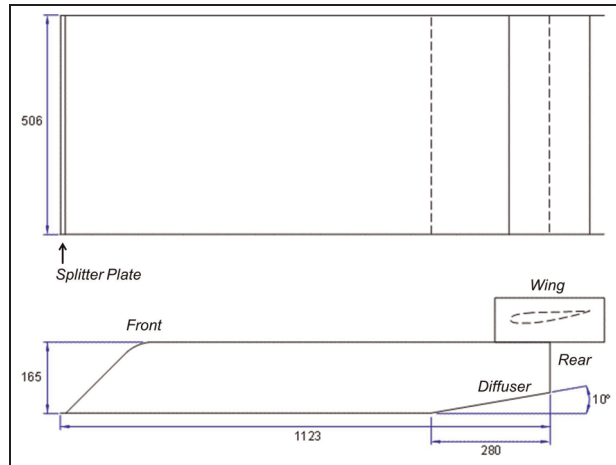


Figure 9. Schematic diagram of the Type C model (dimensions in millimetres), where the flow is from left to right (after Brown⁸).

model results will be primarily compared with the work of Brown.⁸ The results of Wallis and Quinlan⁷ are not included for comparison, as there was a lack of detailed flow information provided on their isolated NASCAR model used.

Front and rear lift comparison. Owing to the comparative complexity of the Type C model, contributions to the front-end lift C_{Lf} and the rear-end lift C_{Lr} will be considered separately. Figure 10 plots the variation from the isolated model case for both the Type C model and the Ahmed model at various ride heights. As in the investigation by Brown,⁸ the front and rear lift of the Ahmed model were assumed to act at the leading edge and the trailing edge of the model, respectively.

At the smallest measured values of z_w , the Ahmed model experienced a rapid increase in both C_L and C_M , as a result of an increase in C_{Lf} . This effect can be seen in Figure 10 for wall distances less than approximately $z_w/L = 0.05$. It is clear that the Type C model also sees a similar increase in C_{Lf} , but at smaller values of z_w , which are found to vary with the ride height. It should be noted that no C_{Lf} increase was found to occur for the Type C model with a 39 mm ride height at the smallest wall distance, although this result arises in part because the magnitude used for the wall distance was too large. Furthermore, the reason for the dip in the front-end lift of the Type C model at lower z_w/L , where C_{Lf} increases for the equivalent Ahmed model case, is believed to be due to the front-end geometry of the Type C model. In this case, the increased pressure over the front end and suction under the front splitter of the Type C model, as the model is brought closer to the wall, increases the front-end downforce. Only at small wall distances ($0.02 < z_w/L < 0.04$) does the Type C model experience an increase in C_{Lf} . This is attributed to the fact that a further reduction in the wall distance causes a greater drop in suction over the top of the front end, than from the underneath of the model. This reduction in suction thus

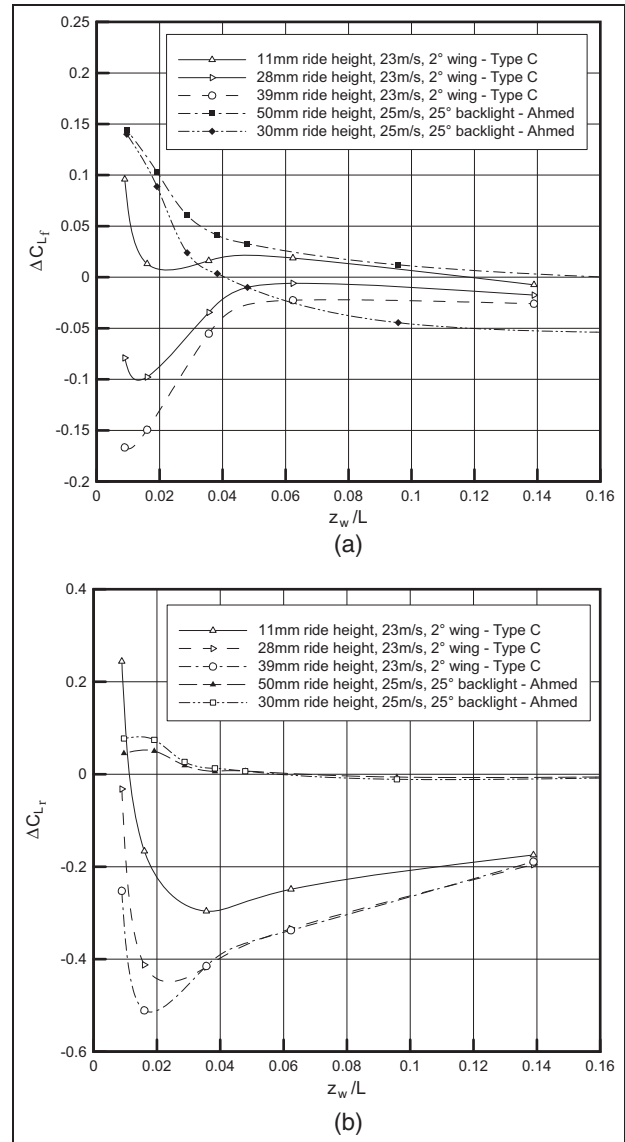


Figure 10. Variations in (a) the front lift and (b) the rear lift with the proximity of the wall and the ride height for the Ahmed model and the Type C car model.

offsets the increased pressure under the bottom of the front end of the car. With increasing ride height, the decreasing wall distance at which this C_{Lf} rise begins, as also found by Brown,⁸ is attributed to the fact that the model boundary layer and resultant pressure distribution restrict the flow under the model.

As was the case for the variation in C_{Lf} shown in Figure 10, the Type C model experienced a greater drop in C_{Lr} with decreasing wall proximity as the ride height was increased. This resulted in minimum measured ΔC_{Lr} values of -0.296 , -0.449 and -0.514 for the 11 mm, 28 mm and 39 mm ride height cases, respectively. As would be expected from the model geometry, the variation in minimum C_{Lr} between the extreme ride height cases of 0.218 for the Type C model is significantly greater than the corresponding variation in minimum C_{Lf} , which is found to be -0.174 between the extreme ride height cases.

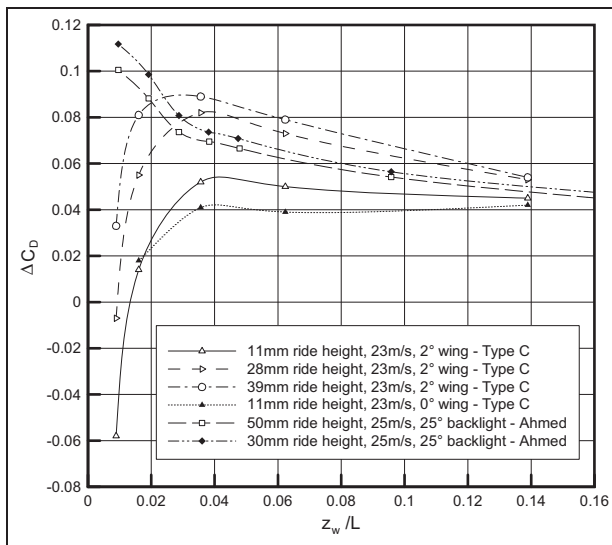


Figure 11. Variation in the drag with the proximity of the wall and the ride height for the Ahmed model and the Type C car model.

It is also clear from Figure 10 that, at the smallest wall distances investigated experimentally, the Type C model experiences a rapid increase in C_{Lr} , for each ride height tested. Again this would be expected to be due to the variation in the contribution of C_{Lr} from the diffuser. At small wall distances, however, the near-side longitudinal vortex strength is reduced and the model boundary layer restricts the flow underneath the model, thus causing the flow to separate from the diffuser, resulting in a large increase in C_p . As was the case for C_{Lf} , the wall distance at which there is a rapid increase in C_{Lr} becomes smaller with increasing ride height. These variations between the minimum and maximum C_{Lr} , measured at each of the ride heights plotted in Figure 10, were 0.245, 0.395 and 0.518 for the 39 mm, 28 mm and 11 mm ride heights, respectively.

Drag comparison. Figure 11 plots the variation in C_D with the wall distance for both the 25° Ahmed model and the Type C model at various ride heights. There is clearly a rapid drop in ΔC_D for the Type C model at the smallest experimentally measured wall distances with each of the ride heights tested. This occurs closer to the wall with increasing ride height, following the trend in ΔC_{Lr} shown in Figure 10. This result emphasises the dominant effect of the diffuser on C_D with the wall distance. In contrast, the Ahmed model, which does not have a diffuser, experiences an increase in the drag with decreasing wall distance for all the cases tested. However, at the points where the Type C model diffuser is no longer producing a significant downforce, at higher ride heights, the Ahmed model exhibits larger values of ΔC_D . At the smallest wall distance and ride height tested by Brown,⁸ there was found to be a significant drop in the model drag from the isolated model case (−0.06, or 9% of the isolated model value). This

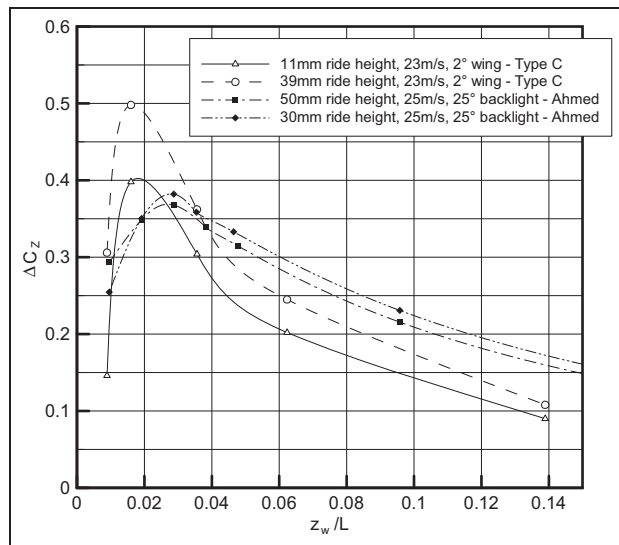


Figure 12. Variation in the side force with the proximity of the wall and the ride height for the Ahmed model and the Type C car model.

illustrates both the sensitivity of the diffuser flow to the proximity of the wall at small ride heights and also the significant drag contribution that this section of the model produces, when in isolation.

The influence of the rear wing on the Type C model is also shown in Figure 11. Only the 11 mm ride height case with a 0° angle of attack is shown for clarity, as a very similar trend is observed for the other ride height cases. In this case, the 0° rear wing case exhibits a smaller increase in ΔC_D than its 2° counterpart. This is attributed to the higher induced drag for the 2° wing than for the 0° wing, with the corresponding increase in ΔC_D .

Side-force comparison. Figure 12 plots the variation in C_Z with the wall distance for both the 25° Ahmed model and the Type C model at various ride heights. Initial inspection shows that both models experience an increase in the side force (towards the wall) as the wall distance falls, before reaching a maximum point with a subsequent step fall in C_Z . It was shown for the Ahmed model that the fact that the pressure drop over the backlight as the wall distance decreased had a significant effect on the side force. For the 25° model, the largest pressure drop and fall in C_p was found to correspond to the maximum value of C_Z . However, the much larger variations in C_{Lr} with the wall distance found for the Type C model than for the Ahmed model indicate that the pressure drop for the underside of the Type C model is significantly greater than with the 25° Ahmed model backlight. Therefore, it is likely that the pressure drop on the near side of the Type C model is greater than that found over the near side of the 25° Ahmed model, resulting in a larger C_Z . It can be seen from Figure 12 that, for wall distances greater than $z_w = 0.04L$, the Ahmed model actually experiences a larger side force than the Type C model does, but that

the Type C maximum values of C_Z are significantly greater than those for the Ahmed model. This can be explained by considering the relative shapes of the model sides.

The Type C model has a much smaller overall side area than the Ahmed model has. If the side areas are considered as a percentage of the corresponding frontal area, then the frontal area of the Type C model's side is 38% of the frontal area of the Ahmed model's side. This would account to some extent for the lower side force experienced by the Type C model at most measured wall distances. Furthermore, a significant proportion of the side area of the Type C model is made up of the wing end plates (approximately 14%). These thin end plates have little frontal blockage and cause a similar drop in C_p with decreasing wall distance. This results in a smaller increase in C_Z with decreasing wall distance for the Type C model than if the side plate area were part of the main body of the model. Therefore, with a maximum fall in C_p near the diffuser leading edge, the side force becomes greater than for the Ahmed model at the same proximity to the wall.

Summary of results comparison

In all the following comparisons, the proximity of the wall appears to reduce the effectiveness of the Type C diffuser to modify the lift and drag. As the lift and drag in this case are dependent on a diffuser vortex pair, as with the Ahmed model, these lift and drag effects correspond to interaction of these vortical structures with the wall boundary layer of similar thickness to the Ahmed model tests. Therefore, we can summarise as follows.

1. The lift increases at most wall distances measured in the case of the Ahmed model, as a result of the increased suction both near the backlight and on the top of the front end. The opposite is found for the Type C model, mainly as a result of increased suction near the underbody diffuser. This continues to a minimum point after which the suction caused by the diffuser is found to drop rapidly, with the subsequent increase in ΔC_L .
2. The drag increases with decreasing wall distance for the Ahmed model, predominantly as a result of the continuing pressure drop on the backlight for the 25° model. The pressure drop caused by the diffuser on the Type C model also results in a drag increase. However, where the diffuser downforce is found to fall rapidly, causing an increase in ΔC_L , there is a corresponding decrease in ΔC_D that is not mirrored by the Ahmed model.
3. The side force acts towards the near side on the Type C and Ahmed model configurations tested. As the pressure drop on the near side and subsequently C_Z are influenced by the increased suction on either the backlight (Ahmed model) or diffuser (Type C model), there is found to be a greater

maximum C_Z value measured for the Type C model.

Conclusions

Force and moment data were presented for an Ahmed reference model in proximity to a side wall. These data were also compared with a previous experimental near-wall study employing a model of a Type C car configuration. In general, the presence of the wall has significant effects on the lift, the drag, the side force and the yawing moment coefficients when compared with the corresponding isolated model cases. With pressure coefficient data and knowledge of the isolated flow characteristics from previous studies, these coefficient changes are, in part, attributed to modification of major vortical structures by the presence of the wall. In particular, there is evidence of the breakdown of longitudinal vortices on the near-wall side of the model, as the wall-to-model distance decreases. This breakdown results in the sharp changes in the lift and the drag coefficients in C_{Lr} and C_D as experienced by the Type C model. A large pressure drop also exists on the near-wall model side in both experimental investigations, which increases in magnitude as the wall-to-model distances decrease. This effect dissipates at wall separations of the same order of magnitude as the expected boundary layer thicknesses.

Owing to the complexity of the expected flow structures, more detailed experimental flow data over the model shapes, with the wall and in isolation, are required before predictions of the effects of the proximity of the wall can be made, as few of these effects are independent of the model geometry.

Funding

This research received no specific grant from any funding agency in the public, commercial or not-for-profit sectors.

References

1. Ahmed SR, Ramm G and Faltin G. Some salient features of the time-averaged ground vehicle wake. SAE paper 840300, 1984.
2. Graysmith JL, Baxendale AJ, Howell JP and Haynes T. Comparisons between CFD and experimental results for the Ahmed reference model. In: *RAeS conference on vehicle aerodynamics*, Loughborough, UK, 18–19 July 1994, pp. 30.1–30.11. London: Royal Aeronautical Society.
3. Aider JL, Dubuc L, Hulin G and Elena L. Experimental and numerical investigation of the flow around a simplified vehicle shape. In: *3rd MIRA international vehicle aerodynamics conference*, Nuneaton, UK, 18–19 October 2000, paper no. 2, session 2. Nuneaton, UK: MIRA.
4. Leinhart H and Becker S. LDA measurements of the flow and turbulence structures in the wake of a simplified car model. Report, Institute of Fluid Mechanics (Lehrstuhl für

- Strömungsmechanik), University Erlangen-Nuremberg, Erlangen, Germany, 2000.
5. Strachan RK, Knowles K and Lawson NJ. Comparisons between CFD and experimental results for a simplified car model in wall proximity. In: *2nd international symposium on integrating CFD and experiments in aerodynamics*, Shrivenham, UK, 5–6 September 2005, paper no. 19. Shrivenham, UK: Cranfield University.
 6. Strachan RK, Knowles K and Lawson NJ. The vortex structure behind an Ahmed reference model in the presence of a moving ground plane. *Exp Fluids* 2007; 42: 659–669.
 7. Wallis SB and Quinlan WJ. A discussion of aerodynamic interference effects between a race car and a race track retaining wall (a wind tunnel NASCAR case study). SAE paper 880458, 1988.
 8. Brown J. *Racecar aerodynamics in close proximity to a retaining wall*. MSc Aerospace Dynamics Individual Thesis, Cranfield University, Cranfield, Bedfordshire, UK, September 2005.
 9. Bertin JJ and Cummings RM. *Aerodynamics for engineers*, 5th edition. London: Pearson Education, 2009.

Appendix

Notation

c	support strut chord = 0.14 m
C_D	drag coefficient = drag force (N)/ qS
C_L	lift coefficient = lift force (N)/ qS
C_M	pitching moment coefficient = pitching moment (N m)/ qSL

C_N	yawing moment coefficient = yawing moment (N m)/ qSL
C_p	pressure coefficient = $(p - p_\infty)/q$
C_R	rolling moment coefficient = rolling moment (N m)/ qSL
C_Z	side-force coefficient = side force (N)/ qS
h	ride height
L	model length = 1.044 m
p	static pressure
p_∞	freestream static pressure
q	freestream dynamic pressure
Re	Reynolds number (based on L)
S	frontal area of the Ahmed model = 0.112032 m ²
t	support strut thickness = 0.0345 m
u_∞	freestream velocity
X	streamwise co-ordinate (see Figure 1)
Y	vertical co-ordinate (see Figure 1)
z_w	distance between the model and the wall
Z	transverse co-ordinate (see Figure 1)
ν	kinematic viscosity
ρ	density of air

Subscripts

f	front
r	rear